

Mesomorphism in columnar phases studied by solid-state nuclear magnetic resonanceSergey V. Dvinskikh,^{1,2} Johan Thaning,² Baltzar Stevansson,² Kjell Jansson,³ Sandeep Kumar,⁴
Herbert Zimmermann,⁵ and Arnold Maliniak^{2,*}¹*Institute of Physics, St. Petersburg State University, 198504 St. Petersburg, Russia*²*Division of Physical Chemistry, Arrhenius Laboratory, Stockholm University, SE-10691 Stockholm, Sweden*³*Division of Inorganic Chemistry, Arrhenius Laboratory, Stockholm University, SE-10691 Stockholm, Sweden*⁴*Raman Research Institute, C. V. Raman Avenue, Bangalore 560 080, India*⁵*Department of Biomedical Optics, Max-Planck-Institut für Medizinische Forschung, Jahnstrasse 29, D-69120 Heidelberg, Germany*

(Received 17 April 2006; published 7 August 2006)

In this paper, we present ¹³C and ¹H NMR investigations of 2, 3, 6, 7, 10, 11-hexahexylthiotriphenylene (HHTT). The measurements were carried out under both static and magic-angle spinning conditions. The phase diagram of HHTT is $K \leftrightarrow H \leftrightarrow D_{hd} \leftrightarrow I$, where H is a helical phase and D_{hd} is a columnar liquid crystal. The motivation was to characterize the molecular order and dynamics and to investigate differences at the molecular level between the two mesophases: H and D_{hd} . It is shown that D_{hd} is a conventional columnar liquid crystal, where the molecular core undergoes fast rotation about the symmetry axis. The orientational order in this mesophase is lower and the temperature dependence of the order parameter is steeper than in other triphenylene-based compounds. On the other hand, in the helical phase the core, similarly to the solid phase, is essentially rigid. The difference between the solid and helical phases is mainly manifested in an increased mobility of the aliphatic chains observed in the latter phase. In addition, the sample exhibits thermal history effects, which are observed in the different behavior upon cooling and heating.

DOI: [10.1103/PhysRevE.74.021703](https://doi.org/10.1103/PhysRevE.74.021703)

PACS number(s): 64.70.Md, 82.56.-b

I. INTRODUCTION

Molecules consisting of a flat, rigid core with laterally attached aliphatic side chains often form columnar phases [1]. The molecular symmetry of these compounds is usually trigonal, although some molecules with lower symmetry also form discotic liquid crystals. The columns, in turn, arrange into two-dimensional (2D) arrays with various symmetries. In addition to a variety of columnar liquid crystals, these types of compounds can also form nematic phases [1]. In general, the phase sequence and the temperature range of the mesomorphic region depend on (i) the size and symmetry of the core; (ii) the length and chemical structure of the side chains, and (iii) the type of the linkage (ether, ester, or thio) between the core and the chains. Over the past 25 years, the mesophases formed by disklike molecules have attracted considerable scientific attention, and to date about 3300 known compounds fall into this category [2]. Several extensive reviews of discotic liquid crystals have been published [1–6].

Nuclear magnetic resonance (NMR) spectroscopy is a powerful experimental tool for studies of solid and liquid crystalline phases [7]. Deuterium (²H) NMR has been used extensively for investigations of the molecular order, structure, and dynamics in columnar mesophases [8–15]. The major advantage of (²H) NMR is that it produces relatively simple spectra that are easy to interpret. An inherent drawback of the method is that it requires isotopic labeling that can be both difficult and expensive. Moreover, the resonance assignment of ²H spectra of molecules containing many different ²H sites is not straightforward [16]. Furthermore,

the ²H NMR line shape reflects the motion of C-D vectors and is, therefore, rather insensitive to details of molecular conformations.

Carbon-13 NMR spectroscopy has several advantages for studying columnar mesophases [17]. Spectra with good signal-to-noise ratios may be obtained in samples with natural isotopic abundance. Resonances from chemically non-equivalent sites are typically well resolved and can often be readily assigned. Anisotropic spin interactions, such as chemical shifts or dipolar couplings, observed in 1D or 2D spectra provide rich information on molecular ordering, structure, and phase transitions [18–22].

In contrast to conventional nematic liquid crystals, columnar phases are usually highly ordered and viscous, which often prevents spontaneous alignment in external fields, particularly in the magnetic field of an NMR spectrometer. The samples can, however, be oriented in strong magnetic fields by slowly cooling from the isotropic liquid. Columnar phases formed by discotic molecules with flat aromatic cores typically align with the columnar axes normal to the field vector. This is a consequence of the negative anisotropy of the magnetic susceptibility of aromatic moieties. Thus, the free energy is minimized for alignment perpendicular to the field. Such alignment results in a planar distribution of domains whose directors are distributed in a plane perpendicular to the field direction.

In this paper, we present ¹³C and ¹H NMR investigations of 2,3,6,7,10,11-hexahexylthiotriphenylene (HHTT), shown in Fig. 1. The experiments are carried out on both stationary and magic angle spinning (MAS) samples. Recently, several experimental studies of HHTT have been reported in the literature [23–37]. This attention can be ascribed to the spectacular charge-transport properties exhibited by this compound [28,29,32,37]. In fact, the charge mobility in HHTT is

*Email address: arnold.maliniak@phyc.su.se

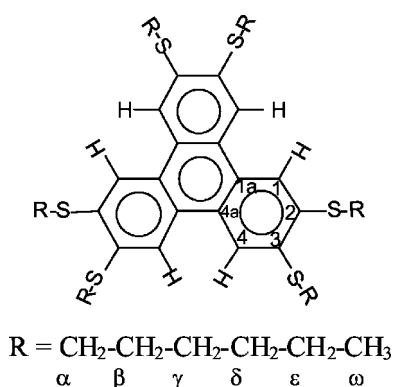
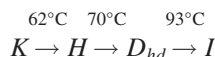


FIG. 1. Schematic of 2,3,6,7,10,11-hexahexylthiotriphenylene (HHTT).

higher than that in any other organic material [27–29]. The phase diagram of HHTT was determined using x-ray and differential-scanning-calorimetry (DSC) techniques [23,24,34,37],



where K and I are the solid and isotropic phases, respectively, and D_{hd} is a hexagonal (h), disordered (d) columnar liquid crystal. The helical (H) phase has also been identified as a columnar D_{ho} liquid crystal [24,26], where the subscript “ o ” denotes ordered phase, and refers to the intracolumnar order of the mesophase. The D_{ho} – D_{hd} transition has been claimed to be unique for HHTT [23,24,26]. Furthermore, it has been suggested that the D_{ho} phase exhibits solid crystalline structure with helical molecular orientational order within the columns [24–26,30]. The molecular description of the D_{ho} and D_{hd} phases has been addressed in several theoretical investigations of HHTT [38–43].

The motivation for the present investigation is to characterize the two mesophases on the molecular level. In particular, we focus on the differences with respect to the molecular order and dynamics.

II. MATERIALS AND METHODS

Materials. The details concerning the preparation of 2,3,6,7,10,11-hexahexylthiotriphenylene (HHTT) were previously described [34].

NMR experiments. All NMR experiments were performed at a magnetic field of 9.4 T on a Chemagnetics Infinity-400 spectrometer at the resonance frequencies of 400 and 100 MHz for protons (^1H) and carbons (^{13}C), respectively. A double/triple-resonance 4 mm magic angle spinning (MAS) probe was used. The measurements were performed either on stationary samples or under MAS condition, where the spinning frequency varied in the range of 1–8 kHz. Heating effects due to sample spinning and radiofrequency irradiation [44] were estimated not to exceed 3 and 2°C, respectively. These effects were not corrected for in the experimental setup.

For the signal enhancement by Hartmann-Hahn cross-polarization (CP) [45,46], the radiofrequency (rf) fields

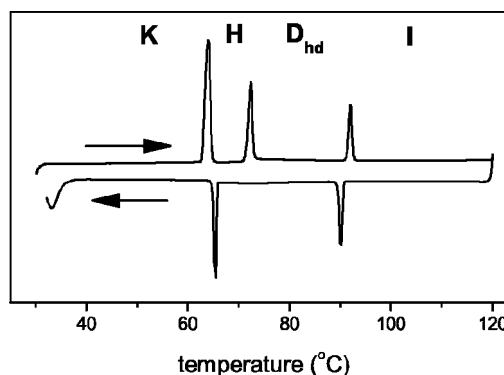


FIG. 2. Differential scanning calorimetry (DSC) thermograms of HHTT.

with nutation frequencies of 40–60 kHz and contact times of 1–3 ms were applied. The heteronuclear decoupling during the detection period in the solid and liquid-crystalline phases was achieved by 70 and 50 kHz TPPM irradiation, respectively [47].

Thermal analysis. Transition temperatures were determined by differential scanning calorimetry (DSC) using a Perkin-Elmer DSC-2C instrument. The temperature and response of heat effects were calibrated by melting of indium. Samples were then investigated in the ranges 30–120°C and 120–30°C, using heating and cooling rates of 5°C min^{−1}.

III. RESULTS AND DISCUSSION

The DSC thermograms of HHTT obtained on heating and cooling are displayed in Fig. 2. Three distinct peaks associated with the endothermic transitions $K \leftrightarrow H$, $H \leftrightarrow D_{hd}$, and $D_{hd} \leftrightarrow I$ are observed at 62, 71, and 92°C and 34, 65, and 90°C for heating and cooling, respectively. These transitions are in good agreement with the values obtained by Maeda and co-workers [34].

A. Stationary sample

1. Carbon-13 NMR spectra

On slow cooling from the isotropic phase, the sample forms a macroscopically oriented hexagonal columnar phase D_{ho} . This procedure results in a planar distribution of columns with the columnar axes aligned perpendicular to the magnetic field. In Fig. 3, a discontinuous shift of line positions at 90°C is observed in the one-dimensional (1D) proton decoupled ^{13}C NMR spectrum. This indicates the isotropic-mesophase transition and is in agreement with the DSC measurement. The six peaks in the aliphatic region correspond to the number of segments in one side chain and indicate the equivalency of the chains in the mesophase. In the aromatic region, three nonequivalent peaks are distinguished, corresponding to the C2, C1a, and C1 carbons; see Fig. 1. Note that the aromatic signals in the columnar mesophase are shifted with respect to the isotropic chemical shifts. Furthermore, there is a shift of these signals within the columnar phase between 90 and 72°C, which reflects the temperature dependence of the orientational order parameter.

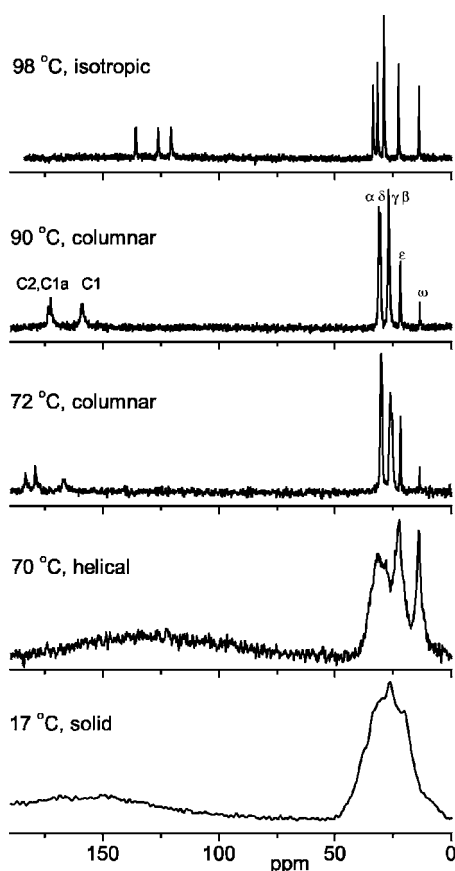


FIG. 3. Carbon-13 NMR spectra of the static HHTT sample as a function of temperature. The NOE and CP enhancement techniques were employed for recording the spectra in the isotropic and other phases, respectively.

The signals in the oriented sample in the liquid crystalline phase correspond to one of the two principal values (δ_{\perp} , δ_{\parallel}) of the partially averaged chemical shift tensor. We identify (see the PASS section below) the aromatic shifts as δ_{\perp} , which indicates that the columns align perpendicular to the magnetic field of the spectrometer. The resonances were assigned on the basis of the two-dimensional (2D) heteronuclear correlation (HETCOR) experiment [48] (not shown), and by observing proton CP dynamics. The aliphatic signals, β and γ , overlapping in the 1D ^{13}C spectrum were resolved in 2D dipolar local field spectra, shown below.

On further cooling, an abrupt change of the ^{13}C line shape takes place between 72 and 70°C, corresponding to the $H \leftrightarrow D_{hd}$ transition. In the helical phase, the signal from the aromatic sites consists of a hump, while the aliphatic peaks are broadened and only partially resolved. This line shape accompanied by additional gradual broadening persists upon further cooling to 17°C. Thus, we conclude that in the helical phase, the aromatic core is rigid (on the NMR time scale) and the motion of the aliphatic chains is significantly restricted. The transition to the solid phase occurs at 17°C, indicating a strong supercooling effect, which is also observed in the DSC diagram, Fig. 2.

The NMR spectral shapes obtained in the solid and columnar phase of HHTT are typical of discotic samples and resemble closely the spectra of the other triphenylene-

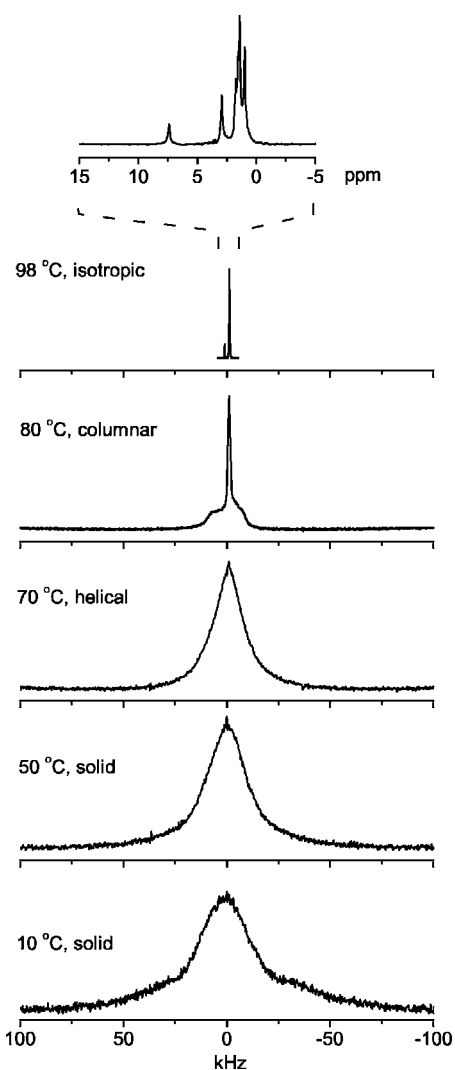


FIG. 4. Temperature dependence of ^1H NMR spectra of the static HHTT sample.

based discotic molecules [17–21,49–52]. The chemical shift values of the carbons bonded to the sulfur atom are, however, significantly different from 2,3,6,7,10,11-hexahexyloxytriphenylene (THE6), an analogous compound in which core and side chains are linked via an ether linkage [17,52].

2. ^1H NMR

The temperature dependence of proton NMR line shapes is displayed in Fig. 4. In the isotropic phase the spectrum is narrow, but broadens significantly upon cooling into the columnar mesophase, which is a result of strong homonuclear dipolar interactions. The relatively narrow central peak in the liquid crystalline phase originates from the mobile outer segments of the side chains, while the broad component is due to the core protons and the protons in the chains with the restricted mobility.

Again, the line shape changes discontinuously at 72°C, where the sample enters the helical phase. The transition from the helical to the solid phase is not sharp, but is merely

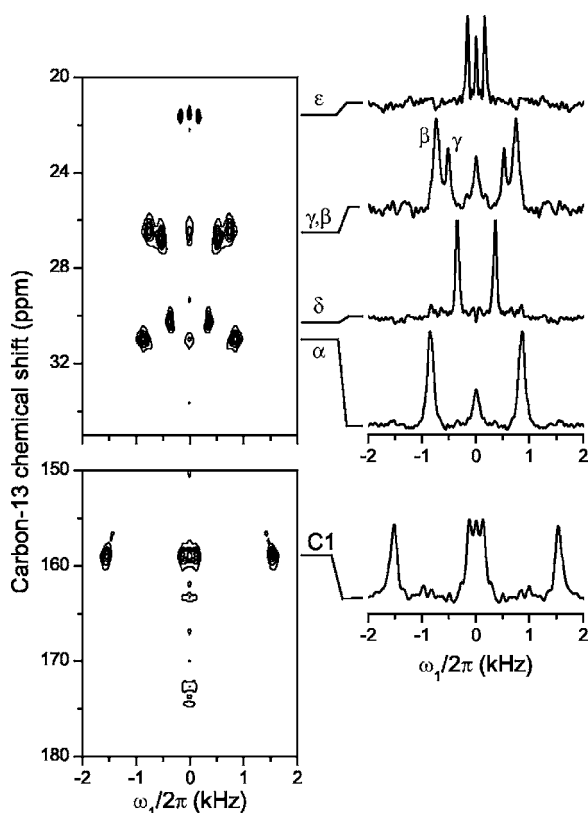


FIG. 5. ^1H - ^{13}C 2D PDLF spectrum in an oriented sample of HHTT at 90°C . The cross sections in the dipolar dimension are shown to the right.

manifested by a gradual broadening of the spectra. The temperature dependence of ^1H NMR line shapes in the oriented static sample is essentially in agreement with the phase behavior observed in ^{13}C spectra.

3. ^1H - ^{13}C 2D local field spectroscopy

The heteronuclear dipolar couplings were measured using the 2D proton encoded separated local field spectroscopy [18,53]. In the following, we use the acronym of the original experiment (PDLF, denoting proton detected local field) where the proton magnetization was observed. In Fig. 5, a 2D PDLF spectrum is displayed, where the ^1H - ^{13}C dipolar splittings in the first (indirectly detected) dimension are correlated with the ^{13}C chemical shift in the second (direct) dimension. The individual slices along the dipolar axis are shown to the right in Fig. 5. Well resolved dipolar doublets produced by the scaled ^1H - ^{13}C dipolar interactions originating from the directly bonded CH pairs were observed for the C1 carbon in the core and for the methylene carbons in the chains. Note that the signals from the α/δ and γ/β sites overlapped in the 1D spectrum (Fig. 3) but are well separated in the dipolar dimension of the 2D PDLF spectrum, due to significantly different ^1H - ^{13}C dipolar couplings.

From the dipolar splitting of the core carbon C1 the orientational order parameter, S_{zz} , for the rigid fragment can be readily estimated from the relationship [54]

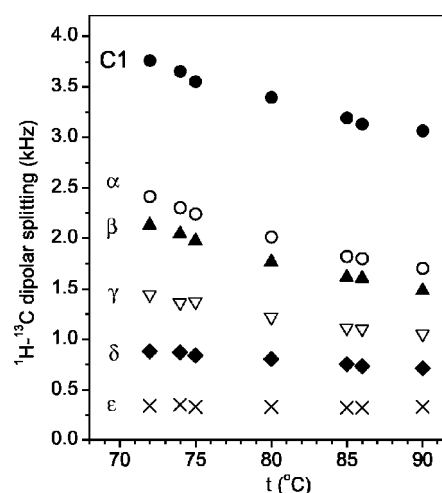


FIG. 6. Temperature dependence of the ^1H - ^{13}C dipolar splittings in the HHTT columnar phase.

$$|\Delta\nu| = \left| \frac{1}{2} k S_{zz} D_{\text{CH}} \right|, \quad (1)$$

where

$$D_{\text{CH}} = - \frac{\mu_0 \gamma_{\text{C}} \gamma_{\text{H}} \hbar}{8 \pi^2 r_{\text{CH}}^3} \quad (2)$$

is the ^1H - ^{13}C dipolar coupling constant for a rigid C-H bond, r_{CH} is the spin-spin distance, and $k=0.424$ is the scaling factor for the homonuclear decoupling sequence BLEW-48 [55] applied in the PDLF experiment. All the other symbols have their usual meaning [54]. The typical value of the dipolar coupling constant for the aromatic site is $D_{\text{CH}} = -21.5$ kHz. The scalar coupling J_{CH} is usually much smaller and therefore neglected. The order parameter derived from Eq. (1) at 90°C (close to the clearing point) and 72°C was $S_{zz} = 0.65$ and 0.80 , respectively. In THE6, the corresponding values derived from the deuterium experiments [8] at 0°C and 20°C from the clearing point were $S_{zz} = 0.89$ and 0.92 . Thus, in the HHTT columnar phase, the order parameter is clearly lower and its temperature dependence is steeper compared to THE6 (see Fig. 6).

In the ^1H - ^{13}C PDLF experiment performed in the helical and solid phase, broad and unresolved lines in both dipolar and chemical shift dimensions were observed, which prevented estimation of dipolar couplings.

B. Magic angle spinning sample

Magic angle sample spinning experiments were performed on a powderlike sample with random director orientation. The sample was prepared by heating to the isotropic phase with subsequent cooling to ambient temperature outside the external magnetic field.

1. Carbon-13 MAS spectra

In Fig. 7, we show the temperature dependence of ^{13}C MAS NMR spectra obtained at 8 kHz spinning frequency. Several signals are observed in the solid phase of the HHTT

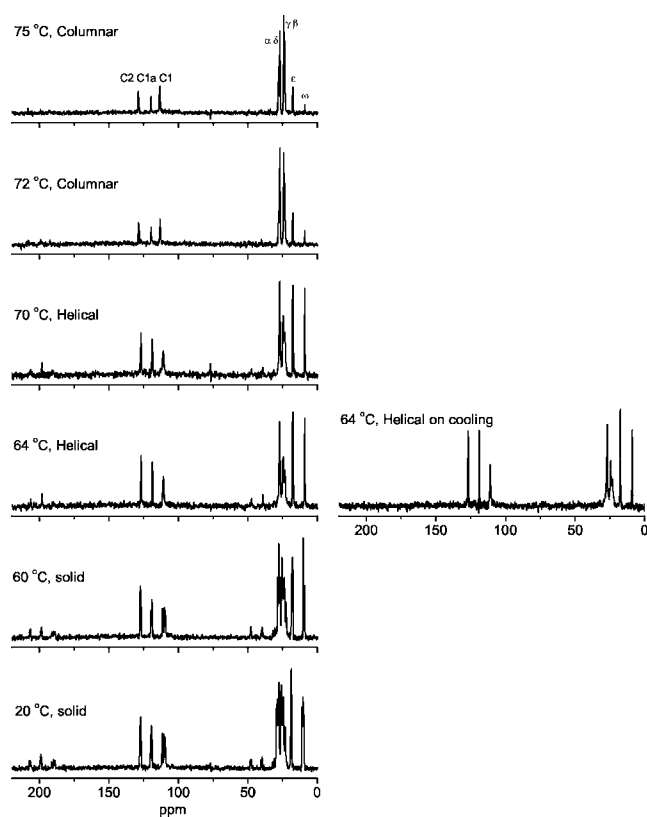


FIG. 7. Carbon-13 MAS NMR spectra obtained at a spinning speed of 8 kHz. Spectra in the left column are recorded on heating. The spectrum obtained in the helical phase by cooling from the columnar liquid crystal is shown to the right. Further cooling to the solid phase resulted in the spectra coinciding with the solid-state spectra in the left column. Note that the signals at ~ 200 and ~ 45 ppm in the solid and helical phases are the side bands.

molecule, which we attribute to the crystallographic non-equivalence of the sites. In particular, the signal of the core carbon, C1, splits into three peaks, but a similar effect was observed for some of the aliphatic signals.

In agreement with the DSC experiments (see Fig. 2), the transition to the helical phase is observed upon heating at 64°C . In this phase, the splittings in the ^{13}C MAS spectra

vanish. Upon further heating into the columnar phase, the intensities of the signals from the core carbons without directly attached protons, C1a and C2, and also the signals from the most mobile groups in the chains, $C\omega$ and $C\epsilon$, are significantly reduced. This reduction originates from an effective averaging of the heteronuclear dipolar couplings due to the fast overall molecular rotation and intensive conformational mobility of outer segments in the chains. The averaging leads to a decreased efficiency of the cross-polarization enhancement, and thus lower intensity of the signals. The spectral shapes are recovered when the sample is cooled from the columnar mesophase to the helical and subsequently to the solid phase. In Fig. 7, we note a difference in the intensities of the aromatic peaks in the helical phase obtained when cooling from the columnar liquid crystal compared to heating from the solid phase.

At relatively fast spinning speed, the 1D ^{13}C MAS spectra are not sensitive to the details of the molecular mobility. It is because fast MAS combined with the heteronuclear decoupling suppresses anisotropic spin interactions. Decreasing the spinning speed enables observation (Fig. 8) of the sideband patterns for the aromatic carbons, which exhibit larger chemical shift anisotropy (CSA) compared to the aliphatic groups. In the following, we use the symbols $H\uparrow$ and $H\downarrow$ to indicate when the helical phase is formed by heating from the solid or cooling from the columnar mesophase, respectively.

The intensities of the sidebands for the aromatic carbons in the $H\uparrow$ phase are very similar to these in the solid phase. In addition, no dramatic change in the distribution of the sideband intensities is observed upon further heating to the columnar phase. This is expected, since the axis of the molecular rotation in the columnar phase nearly coincides with the main principal axis of the CSA tensor for the aromatic core. Hence, the molecular rotation in the mesophase results merely in an averaging of the asymmetry of the CSA, while the anisotropy of the CSA is scaled with an order parameter. Interestingly, there is a significant difference in the sideband pattern observed in the $H\uparrow$ and $H\downarrow$ phases; see Fig. 8. In particular, the central band intensity increases at the expense of decreasing intensities of the sidebands. This can, in principle, be attributed to (i) fast but axially asymmetric molecu-

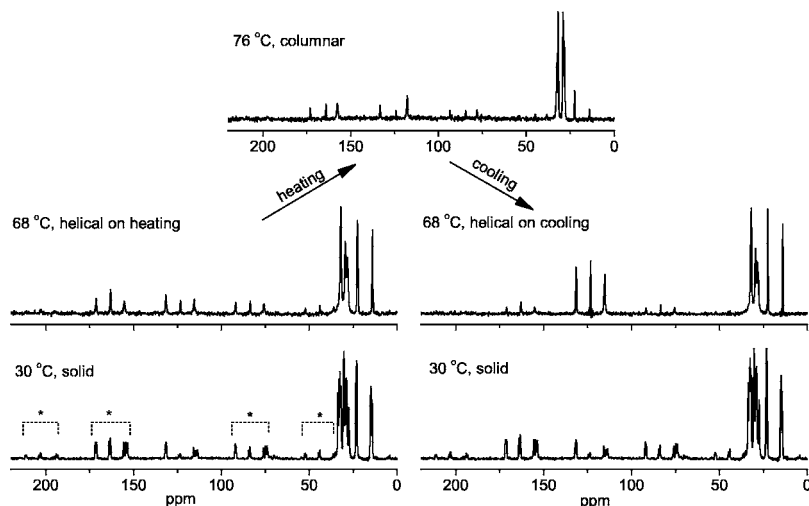


FIG. 8. ^{13}C MAS NMR spectra recorded at a spinning frequency of 4 kHz. Asterisks indicate sidebands.

TABLE I. Experimental values of the chemical shift tensor parameters $\Delta\delta^p$ (in ppm) and η^p for the core carbons in HHTT.

$T(^{\circ}\text{C})$	Phase	C1a		C1		C2	
		$\Delta\delta$	η	$\Delta\delta$	η	$\Delta\delta$	η
60	Solid	-128	0.42	-100	0.76	-95	0.73
68	Helical H \uparrow	-126	0.42	-90	0.85	-91	0.77
68	Helical H \downarrow	-41	0.92	+42	0.84	+39	0.94
76	Columnar	-120	0	-101	0	-100	0

lar mobility resulting from restricted rotations, (ii) molecular rotation with the rate comparable to or slower than the CSA coupling constant, and (iii) a combination of (i) and (ii). Such a sideband pattern persists in the whole temperature range of the H \downarrow phase, and transforms to the conventional shape at the transition to the solid phase.

2. 2D PASS spectra

The ^{13}C chemical shift tensor parameters for the aromatic carbons were determined using the slow MAS (spinning frequency of 2 kHz) 2D PASS technique [56]. The CSA tensor may be characterized by its anisotropy

$$\Delta\delta^p = \delta_{zz}^p - (\delta_{xx}^p + \delta_{yy}^p)/2, \quad (3)$$

where δ_{zz}^p denotes the principal component furthest away from the isotropic chemical shift $\delta_{\text{iso}} = (\delta_{xx}^p + \delta_{yy}^p + \delta_{zz}^p)/3$, and the asymmetry parameter is given by

$$\eta^p = (\delta_{xx}^p - \delta_{yy}^p)/(\delta_{zz}^p - \delta_{\text{iso}}). \quad (4)$$

The experimental values for $\Delta\delta^p$ and η^p are collected in Table I. Parameters determined in the solid phase were essentially independent of temperature and the thermal history of the sample.

Upon heating to the helical phase, there was no significant change in the CS parameters. Further heating to a conventional columnar phase resulted in an axially symmetric chemical shift tensor. In a uniaxial mesophase, in the presence of the fast molecular rotations, the rigid-lattice CSA

tensor is transformed into an effectively averaged axially symmetric tensor with the principal components δ_{\parallel} and δ_{\perp} . Liquid crystalline domains with the director oriented parallel and perpendicular to the magnetic field exhibit the chemical shifts δ_{\parallel} and δ_{\perp} , respectively.

Cooling back to the helical phase (i.e., H \downarrow phase) produced unexpected results. A strongly asymmetric chemical shift tensor with reduced anisotropy parameter was obtained. These results were well reproduced by repeating the measurements for several heating/cooling cycles.

3. ^1H MAS Spectra

The phase transitions solid-helical and helical-columnar are observed in ^1H MAS spectra shown in Fig. 9. The proton signal in the solid and helical phases, observed at 8 kHz spinning frequency, is split into partially resolved dipolar sidebands. At the transition from the solid to helical phase, the intensity of the central band increases drastically. This can be attributed to the onset of the conformational transitions in the side chains. The homogeneous broadening due to strong homonuclear dipolar interactions prevents resolution of nonequivalent proton signals in the solid and helical phases. In contrast, the ^1H lines in the columnar phase are much narrower, hence aliphatic and aromatic signals are resolved.

Even more dramatic spectral changes at phase transitions are observed at lower spinning rates. Essentially no sidebands are resolved in the solid phase at 4 kHz (see Fig. 9, right column), whereas partially resolved sideband spectral structure is obtained in the helical phase, and highly resolved spectra are detected in the columnar phase.

In contrast to ^{13}C MAS NMR spectra at the spinning frequency of 4 kHz, there was no detectable difference in the spectral shapes of H \uparrow and H \downarrow . This is due to the poorly resolved sideband pattern in the proton spectra in the helical phase.

4. ^1H - ^{13}C 2D local field spectroscopy

To estimate the heteronuclear dipolar couplings in powder samples, two types of 2D MAS separated local field experi-

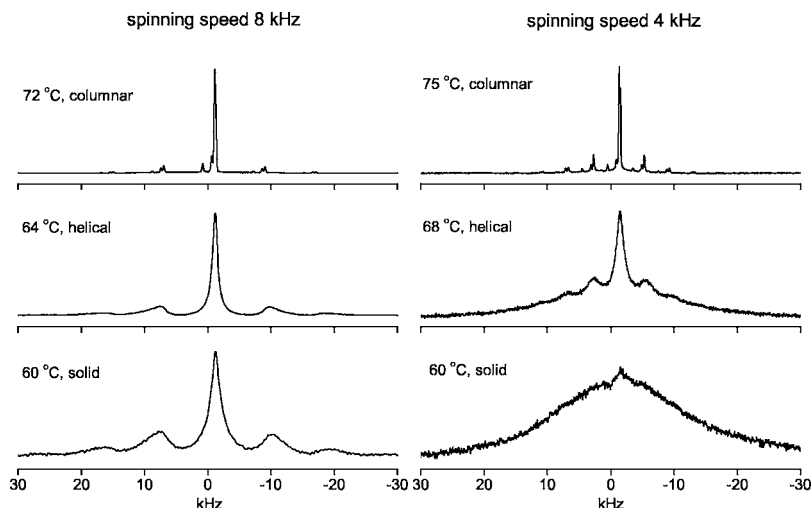


FIG. 9. ^1H MAS NMR spectra obtained at 8 (left) and 4 kHz (right) spinning frequency.

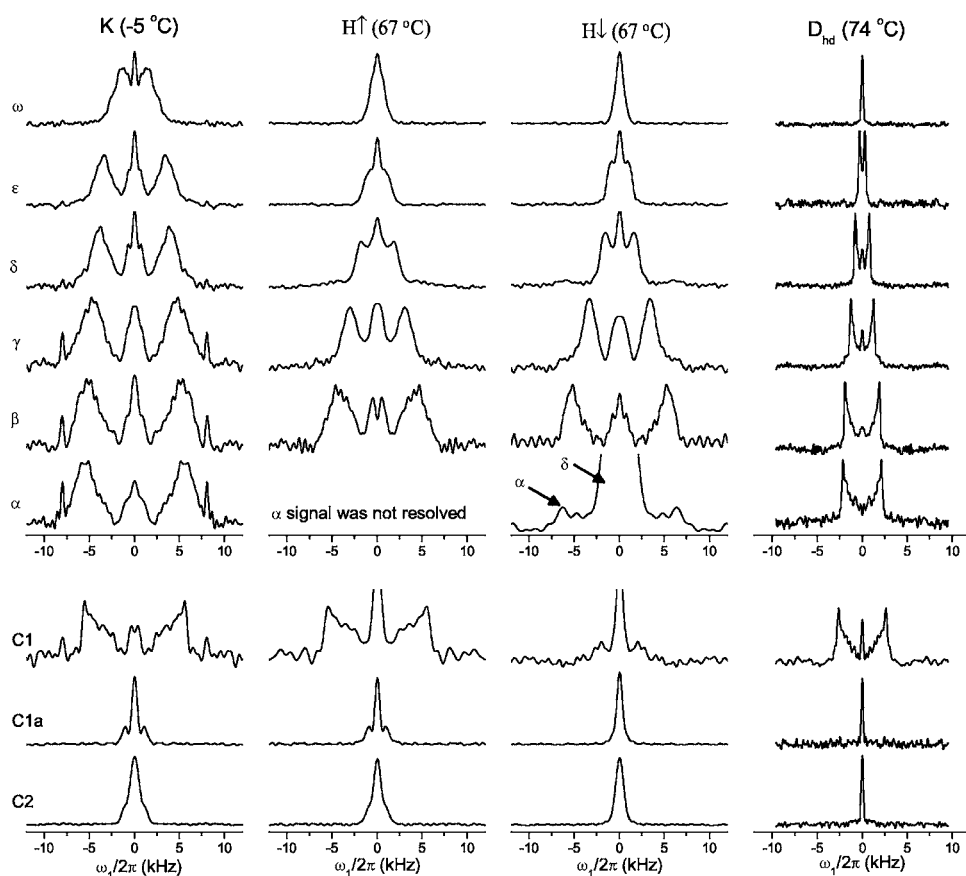


FIG. 10. ^{13}C - ^1H FSLG-CP dipolar spectra obtained in the solid phase (first column), helical phases (second and third column), and columnar phase (last column). Spinning frequency is 8 kHz. The assignment of the aliphatic signals in the solid and helical phases is tentative, based on the strength of the dipolar splittings. The aliphatic signals are shown in the order of the segment number along the chains.

ments were performed: FSLG-CP [50,51,57,58] and R-PDLF [22,58]. The results from the two methods were essentially identical, and the discussion below is therefore restricted to the FSLG-CP experiments.

Dipolar spectra measured in the solid phase (Fig. 10, left column) indicate that (i) the core is immobile; (ii) inner methylene groups in the chains are immobile, and (iii) methyl group and outer methylenes (δ and ε) exhibit partial mobility. In particular, the dipolar splitting of the ε -carbon is reduced by a factor of 0.6, as compared to that expected in the rigid solid. The dipolar couplings measured in the solid phase in a wide temperature range, from -5 to 60 °C, remained essentially constant except for the ε -methylenes and terminal ω -methyls, which exhibited decreasing couplings at the elevated temperature.

In the columnar phase, the dipolar splittings for all sites, including the C1 carbon, decrease by at least a factor of 2 (Fig. 10, right column), compared to these in the solid phase. This is a manifestation of the fast molecular rotation around the molecular symmetry axis. Note that the dipolar coupling for the C1 carbon in the static sample (Fig. 5) is reduced by an additional factor of 2, due to the director orientation perpendicular to the magnetic field. The molecular order parameter $S_{zz}=0.8$ (at 74 °C) can be derived from the dipolar splitting of the C1 carbon signal, assuming fast molecular rotation around the axis perpendicular to the core plane. This is in agreement with the value obtained in the oriented static HHTT sample at this temperature (see above).

The dipolar spectra determined for $\text{H}\downarrow$ and $\text{H}\uparrow$ are shown in the two middle columns of Fig. 10. Five important fea-

tures are characteristic for these spectra: (i) The splittings decreased slightly compared to the solid phase, indicating an increased mobility; (ii) in $\text{H}\uparrow$, the dipolar splitting of C1 is similar to that in the solid phase, thus the aromatic core remains immobile in the helical phase; (iii) the splittings of the methylene signals are similar for $\text{H}\downarrow$ and $\text{H}\uparrow$; (iv) the signal from the α -carbon in the aliphatic chain is not resolved in $\text{H}\uparrow$; and (v) no dipolar splitting is observed for the core carbon C1 in $\text{H}\downarrow$. We attribute the last two observations to the fact that the dynamic processes occur on the time scale $\tau_c \approx 10^{-3} - 10^{-4}$ s comparable to the spinning speed and the reciprocal value of the dipolar coupling and CSA interaction.

IV. SUMMARY AND CONCLUSIONS

Several previously reported investigations of 2,3,6,7,10,11-hexahexylthiotriphenylene (HHTT) argue about the nature of the two mesophases between the solid and isotropic phase. In particular, the low-temperature phase denoted here as helical (H) has also been characterized as a columnar liquid crystal, D_{ho} [23,24,26,41]. Furthermore, a number of studies have focused on the phase transition $D_{ho} \leftrightarrow D_{hd}$ [24,42,43].

We have shown here, based on ^{13}C and ^1H NMR investigations, that while the high-temperature mesophase is a conventional columnar liquid crystal D_{hd} , the low-temperature phase denoted H is a solid phase. This conclusion is based on the assumption that in the columnar phase, the molecular core undergoes fast rotation about the symmetry axis, whereas it is essentially rigid in the solid state. The differ-

ence between the solid and helical phases is mainly manifested in an increased mobility of the aliphatic chains observed in the latter phase. The temperature dependence of the NMR spectra was in very good agreement with the phase diagram determined by the differential scanning calorimetry (DSC).

Planar rotation about the molecular symmetry axis, characteristic of the columnar liquid crystals, was clearly observed in the high-temperature phase, D_{hd} , of HHTT. This rotation is fast, on the NMR time scale, which is defined by the strength of the anisotropic spin interactions (dipolar and CSA) of the order of $\sim 10^{-4}$ s. The orientational order of the core fragment in the columnar mesophase is significantly lower and its temperature dependence is stronger than in similar compounds. The fast molecular rotation in columns is manifested in several experimental observations. (i) ^{13}C spectra of the static sample (Fig. 3) exhibit, in contrast to the helical and solid phases, narrow peaks, and the chemical shifts of the aromatic carbons correspond to the principal component of the chemical shift tensor perpendicular to the normal to the core plane. (ii) The width of the static ^1H spectrum (Fig. 4) is reduced by more than a factor of 2 compared to the helical and solid phases. (iii) The dipolar ^1H - ^{13}C coupling for the core carbon C1 (Figs. 5 and 10) is also reduced by a factor of 2 compared to an immobile C-H bond. Note that the coupling derived from the static sample spectra (Fig. 5) is reduced by an additional factor of 2, due to the perpendicular orientation of the columns. (iv) The CP efficiency for the nonprotonated sites, C2 and C1a, under MAS condition was significantly reduced, see Fig. 7. (v) Finally, well resolved sideband structure of the ^1H MAS spectrum obtained at low spinning speed is indicative of inhomogeneous-like behavior of the homonuclear proton interactions [59]. This is a typical result from the collinear directions of all motionally averaged H-H vectors projected onto the molecular rotation axis and is a consequence of the

identical angular dependence of the average dipolar interactions with respect to the external magnetic-field direction [59].

Similar parameters for the anisotropic spin interactions were found in the solid and helical phases. However, a change in the molecular arrangement in the crystal lattice occurs at the solid-to-helical phase transition, as suggested by the disappearance of the fine splittings of the ^{13}C MAS spectral peaks; see Fig. 7. Hence, the molecular structural nonequivalence, present in the solid phase, vanishes in the helical phase. This structural rearrangement may become possible due to an increased mobility of the outer parts of the side chains, allowing for relaxing of some lattice packing constraints.

Another interesting experimental observation is the difference between the spectral characteristics in the helical phases: $\text{H}\downarrow$ and $\text{H}\uparrow$. The significant change of the parameters of the chemical shift tensor and the ^1H - ^{13}C dipolar interaction in $\text{H}\downarrow$ as compared to the solid phase and also to the $\text{H}\uparrow$ phase can be explained by the presence of the restricted molecular reorientations and/or slow molecular motion. Clearly, fast and unrestricted molecular rotation characteristic of the liquid crystalline phase is ruled out, based on the arguments presented above.

To get further insight into the molecular dynamics of the helical phase, slow exchange 2D NMR experiments will be carried out. Particularly, the 2D MAS exchange CODEX [60] experiment can provide detailed information on the time scale of the molecular motion in the range of $\sim 10^{-3}$ – 10^0 s.

ACKNOWLEDGMENTS

This work was supported by the Swedish Research Council, the Carl Trygger Foundation, the Magn. Bergvall Foundation, DAAD, and the Russian Foundation for Basic Research (Grant No. 04-03-32639).

-
- [1] S. Chandrasekhar and G. S. Ranganath, *Rep. Prog. Phys.* **53**, 57 (1990).
 [2] S. Kumar, *Liq. Cryst.* **31**, 1037 (2004).
 [3] S. Chandrasekhar, *Liq. Cryst.* **14**, 3 (1993).
 [4] D. Demus, J. Goodby, G. W. Gray, H.-W. Spiess, and V. Vill, *Handbook of Liquid Crystals* (Wiley-VCH, Weinheim, 1998).
 [5] K. Praefcke and A. Eckert, *Mol. Cryst. Liq. Cryst.* **396**, 265 (2003).
 [6] S. Kumar, *Liq. Cryst.* **32**, 1089 (2005).
 [7] K. Schmidt-Rohr and H. W. Spiess, *Multidimensional Solid-State NMR and Polymers* (Academic Press, London, 1994).
 [8] D. Goldfarb, Z. Luz, and H. Zimmermann, *J. Chem. Phys.* **78**, 7065 (1983).
 [9] Z. Luz, D. Goldfarb, and H. Zimmermann, in *Nuclear Magnetic Resonance of Liquid Crystals*, edited by J. W. Emsley (Reidel, Dordrecht, 1985), p. 343.
 [10] R. Y. Dong, *Isr. J. Chem.* **23**, 370 (1983).
 [11] R. Y. Dong and C. R. Morcombe, *Liq. Cryst.* **27**, 897 (2000).
 [12] M. Werth, J. Leisen, C. Boeffel, R. Y. Dong, and H. W. Spiess, *J. Phys. II* **3**, 53 (1993).
 [13] A. Maliniak, S. Greenbaum, R. Poupko, H. Zimmermann, and Z. Luz, *J. Phys. Chem.* **97**, 4832 (1993).
 [14] D. Sandström, M. Nygren, H. Zimmermann, and A. Maliniak, *J. Phys. Chem.* **99**, 6661 (1995).
 [15] S. Zamir, R. Poupko, Z. Luz, B. Huser, C. Boeffel, and H. Zimmermann, *J. Am. Chem. Soc.* **116**, 1973 (1994).
 [16] D. Sandström and H. Zimmermann, *J. Phys. Chem. B* **104**, 1490 (2000).
 [17] S. V. Dvinskikh, D. Sandström, H. Zimmermann, and A. Maliniak, *Prog. Nucl. Magn. Reson. Spectrosc.* **48**, 85 (2006).
 [18] S. V. Dvinskikh, H. Zimmermann, A. Maliniak, and D. Sandström, *J. Magn. Reson.* **163**, 46 (2003).
 [19] S. V. Dvinskikh, Z. Luz, H. Zimmermann, A. Maliniak, and D. Sandström, *J. Phys. Chem. B* **107**, 1969 (2003).
 [20] S. V. Dvinskikh, D. Sandström, Z. Luz, H. Zimmermann, and A. Maliniak, *J. Chem. Phys.* **119**, 413 (2003).
 [21] S. V. Dvinskikh, D. Sandström, H. Zimmermann, and A. Maliniak, *Chem. Phys. Lett.* **382**, 410 (2003).

- [22] S. V. Dvinskikh, H. Zimmermann, A. Maliniak, and D. Sandström, *J. Magn. Reson.* **168**, 194 (2004).
- [23] E. F. Gramsbergen, H. J. Hoving, W. H. de Jue, K. Praefcke, and B. Kohne, *Liq. Cryst.* **1**, 397 (1986).
- [24] E. Fontes, P. A. Heiney, and W. H. de Jeu, *Phys. Rev. Lett.* **61**, 1202 (1988).
- [25] S. H. J. Idziak, P. A. Heiney, J. P. McCauley, P. Carroll, and A. B. Smith, *Mol. Cryst. Liq. Cryst. Sci. Technol., Sect. A* **237**, 271 (1993).
- [26] P. A. Heiney, E. Fontes, W. H. de Jue, A. Riera, P. Carroll, and A. B. Smith, *J. Phys. (Paris)* **50**, 461 (1989).
- [27] G. B. M. Vaughan, P. A. Heiney, J. P. McCauley, and A. B. Smith, *Phys. Rev. B* **46**, 2787 (1992).
- [28] D. Adam, P. Schuhmacher, J. Simmerer, L. Häussling, K. Siemensemeyer, K. H. Eitzbach, H. Ringsdorf, and D. Haarer, *Nature (London)* **371**, 141 (1994).
- [29] V. S. K. Balagurusamy, S. K. Prasad, S. Chandrasekhar, S. Kumar, M. Manickam, and C. V. Yelamaggad, *Pramana* **53**, 3 (1999).
- [30] S. Marguet, D. Markovitsi, P. Millie, H. Sigal, and S. Kumar, *J. Phys. Chem. B* **102**, 4697 (1998).
- [31] T. Perova, S. Tsvetkov, J. Vij, and S. Kumar, *Mol. Cryst. Liq. Cryst. Sci. Technol., Sect. A* **351**, 95 (2000).
- [32] J. Bondkowski, I. Bleyl, D. Haarer, and D. Adam, *Chem. Phys. Lett.* **283**, 207 (1998).
- [33] R. Bilke, A. Schreiber, I. Bleyl, D. Haarer, and D. Adam, *J. Appl. Phys.* **87**, 3872 (2000).
- [34] Y. Maeda, D. S. S. Rao, S. K. Prasad, S. Chandrasekhar, and S. Kumar, *Liq. Cryst.* **28**, 1679 (2001).
- [35] A. N. Cammidge and H. Gopee, *J. Mater. Chem.* **11**, 2773 (2001).
- [36] A. M. van de Craats, M. P. de Haas, and J. M. Warman, *Synth. Met.* **86**, 2125 (1997).
- [37] S. Chandrasekhar and V. S. K. Balagurusamy, *Proc. R. Soc. London, Ser. A* **458**, 1783 (2002).
- [38] M. L. Plumer, A. Caille, and O. Heinonen, *Phys. Rev. B* **47**, 8479 (1993).
- [39] T. Horiguchi and Y. Fukui, *Phys. Rev. B* **50**, 7140 (1994).
- [40] M. Hebert, *Phys. Rev. E* **55**, 7063 (1997).
- [41] G. Lamoureux, A. Caille, and D. Senechal, *Phys. Rev. E* **58**, 5898 (1998).
- [42] J. G. Demers and A. Caille, *Phys. Rev. E* **65**, 062701 (2002).
- [43] J. G. Demers and A. Caille, *Phys. Rev. E* **67**, 011707 (2003).
- [44] S. V. Dvinskikh, V. Castro, and D. Sandström, *Magn. Reson. Chem.* **42**, 875 (2004).
- [45] S. R. Hartmann and E. L. Hahn, *Phys. Rev.* **128**, 2042 (1962).
- [46] A. Pines, M. G. Gibby, and J. S. Waugh, *J. Chem. Phys.* **59**, 569 (1973).
- [47] A. E. Bennett, C. M. Rienstra, M. Auger, K. V. Lakshmi, and R. G. Griffin, *J. Chem. Phys.* **103**, 6951 (1995).
- [48] D. P. Burum and A. Bielecki, *J. Magn. Reson. (1969-1992)* **94**, 645 (1991).
- [49] V. Rutar, R. Blinc, M. Vilfan, A. Zann, and J. C. Dubois, *J. Phys. (Paris)* **43**, 761 (1982).
- [50] S. V. Dvinskikh, H. Zimmermann, A. Maliniak, and D. Sandström, *J. Magn. Reson.* **164**, 165 (2003).
- [51] S. V. Dvinskikh, H. Zimmermann, A. Maliniak, and D. Sandström, *J. Chem. Phys.* **122**, 044512 (2005).
- [52] S. V. Dvinskikh, K. Yamamoto, and A. Ramamoorthy, *Chem. Phys. Lett.* **419**, 168 (2006).
- [53] B. M. Fung, K. Ermolaev, and Y. Yu, *J. Magn. Reson.* **138**, 28 (1999).
- [54] R. Y. Dong, *Nuclear Magnetic Resonance of Liquid Crystals* (Springer, New York, 1994).
- [55] D. P. Burum, M. Linder, and R. R. Ernst, *J. Magn. Reson. (1969-1992)* **44**, 173 (1981).
- [56] O. N. Antzutkin, *Prog. Nucl. Magn. Reson. Spectrosc.* **35**, 203 (1999).
- [57] S. V. Dvinskikh and D. Sandström, *J. Magn. Reson.* **175**, 163 (2005).
- [58] S. V. Dvinskikh, V. Castro, and D. Sandström, *Phys. Chem. Chem. Phys.* **7**, 607 (2005).
- [59] M. M. Maricq and J. S. Waugh, *J. Chem. Phys.* **70**, 3300 (1979).
- [60] E. R. de Azevedo, W.-G. Hu, T. J. Bonagamba, and K. Schmidt-Rohr, *J. Am. Chem. Soc.* **121**, 8411 (1999).